Fatty Acid Binding Proteins

Deutsche Ausgabe: DOI: 10.1002/ange.201601326
Internationale Ausgabe: DOI: 10.1002/anie.201601326

Local Unfolding of Fatty Acid Binding Protein to Allow Ligand Entry for Binding

*Tianshu Xiao, Jing-song Fan, Hu Zhou, Qingsong Lin, and Daiwen Yang**

Abstract: *Fatty acid binding proteins are responsible for the transportation of fatty acids in biology. Despite intensive studies, the molecular mechanism of fatty acid entry to and exit from the protein cavity is still unclear. Here a cap-closed variant of human intestinal fatty acid binding protein was generated by mutagenesis, in which the helical cap is locked to the β-barrel by a disulfide linkage. Structure determination shows that this variant adopts a closed conformation, but still uptakes fatty acids. Stopped-flow experiments indicate that a rate-limiting step exists before the ligand association and this step corresponds to the conversion of the closed form to the open one. NMR relaxation dispersion and H-D exchange data demonstrate the presence of two excited states: one is native-like, but the other adopts a locally unfolded structure. Local unfolding of helix 2 generates an opening for ligands to enter the protein cavity, and thus controls the ligand association rate.*

Fatty acid binding proteins (FABPs) belong to the intracellular lipid binding protein family, featured with a conserved β-barrel structure capped by two helices.[1] They assist the transportation of long-chain fatty acids, which are responsible for multiple biological activities such as energy supply, lipid metabolism, signal transduction, and precursor synthesis.[2] Furthermore, FABPs have been found to be involved in some metabolic diseases such as insulin resistance and diabetes, suggesting an additional role other than the role as the chaperone of lipid transportation.[2] Despite the important and diverse roles of FABPs and intensive studies in their structures and dynamics, how fatty acids enter the cavity remains obscure. The helical portal region, consisting of helix α2 and β turns C-D and E-F (Figure 1 A), has been hypothesized as the entrance to the internal binding site.[3,4] The same region has also been proposed as the exit of ligands.[3–5] The hypothesis is supported by a helix-less variant of rat intestinal FABP (IFABP), which has a large opening and displays very different ligand binding kinetics from the wild-type protein.[6] However, nearly all structures of ligand-free and -bound wild type FABPs obtained in both crystal and solution states show no obvious openings for ligand entry or exit.[3,7–11] Thus, minor or "invisible" states with the opening, which are in conformational reorganizations with the native close state, must play a critical role in ligand association and dissociation. The minor open state might have a cap-open conformation, as the helical cap was not shut tightly over the entrance to the β-barrel in the only structure of rat liver FABP.[12] So far, however, the existence of such a minor state has not yet been experimentally confirmed. Conformational exchanges are evident from NMR relaxation studies on FABPs,[13–16] but the structural changes seem not to be restricted to the portal region. Moreover, the rate from the closed state to the open state derived from NMR data was found to be much smaller than the ligand association rate.[16] Therefore, the conformational exchanges observed so far are very likely irrelevant to the ligand association.

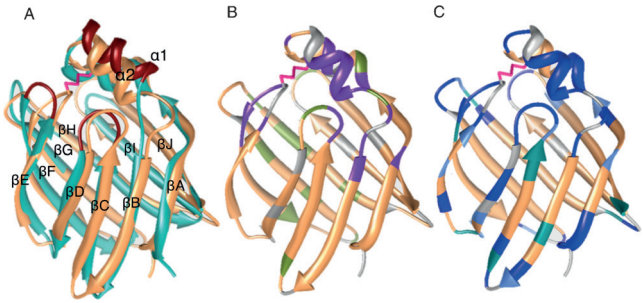

Figure 1. A) Structure comparison of hIFABP (PDB ID: 3IFB; cyan) and its variant (sandy brown), B) distribution of residues showing three states (purple) and two states (sandy brown), and C) distribution of amides with different H-D exchange protection factors (blue: $P<100$; light blue: $100\le P\le 1000$; cyan: $10^3<P\le 10^4$; sandy brown: $P>10^4$). In (A), helical portal region is highlighted in dark red. In (B) and (C), the residues whose data were unavailable are colored in gray. In (B), the residues displaying no obvious relaxation dispersion are labeled in olive green. The disulfide linkage is shown in pink.

To investigate if the open state is achieved through moving the cap (formed by the two helices) away from the barrel's entrance, a cap-closed variant of human intestinal FABP (hIFABP) was generated by mutating K27 located in α2 and D74 in β-turn E-F into cysteine (Figure 1 A). The presence of a disulfide bond between the two cysteine residues is supported by significant difference of ^{1}H–^{15}N correlation spectra in the absence and presence of reducing agent DTT (Supporting Information, Figure S1). The $^{13}C_{\beta}$ chemical shifts of C27 (42.2 ppm) and C74 (41.5 ppm), which are typical for oxidized cysteine, further validate the formation of a disulfide bond. The structure of the variant was determined using triple resonance NMR experiments (Supporting Information, Table S1 and Figure S2).[17,18] The variant adopts a similar structure to the wild-type protein (Figure 1 A). The second helix is well-defined and its RMSD is slightly larger than that of the first helix in 20 best structures (Supporting Information, Figure S2), which is different from what was observed in the NMR structure of

[*] T. Xiao, Dr. J. Fan, H. Zhou, Dr. Q. Lin, Prof. D. Yang
Department of Biological Sciences, National University of Singapore
14 Science Drive 4, Singapore 117543 (Singapore)
E-mail: dbsydw@nus.edu.sg

Supporting information for this article can be found under: http://dx.doi.org/10.1002/anie.201601326.

rat IFABP.[4] The intramolecular disulfide bond pulls the second helix closer to β-turn E-F by about 1.4 Å, resulting in small differences in the orientations of strands B, C, and D and helices 1 and 2 in comparison to the wild-type protein structure. Because of the disulfide linkage, the cap is always locked with the entrance to the barrel, eliminating the minor open states in which the helical cap is far away from β-turns E-F and C-D.

Although the variant has a locked cap, it still bound oleic acid. Its affinity was 0.79 μM, circa 10 times smaller than that of the wild type protein (0.08 μM) as determined by fluorescence titration (Supporting Information, Figure S3). The result indicates that an "invisible" open state still exists in the cap-closed variant since it can uptake ligands, and the opening should not be achieved by simply moving the cap up and down because the cap is already locked.

To examine the effect of the disulfide bond on ligand binding kinetics, we performed stopped-flow experiments under the pseudo first-order reaction condition (that is, the ligand is in excess relative to the protein).

For both the wild-type and mutant hIFABP, the stopped-flow curves were fitted very well with a double exponential function rather than a single exponential function (Supporting Information, Figures S4 and S5), indicating the ligand binding occurs in at least two steps: one fast and one slow. The apparent association rates for the fast step increased linearly with ligand concentrations in the initial stage, indicating that this step is the oleic acid binding step. A further increase of the ligand concentration led to a plateau for the fast association rate (Figure 2; Supporting Information, Figure S6), showing the presence of a rate-limiting step before

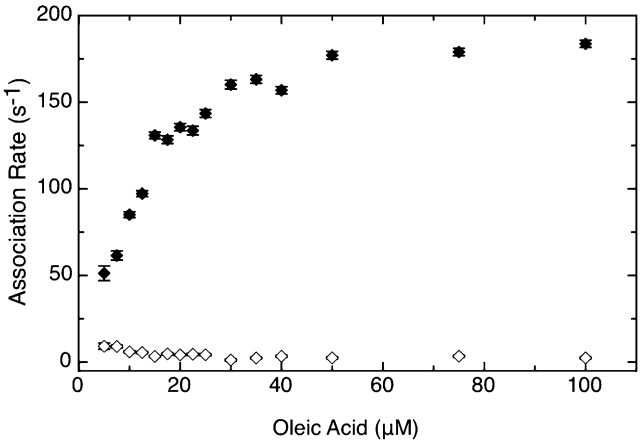

Figure 2. Dependences of apparent association rates for the fast (◆) and slow (◇) steps on ligand concentrations.

the ligand association step. The rate-limiting step may correspond to the conformational exchange from a closed state to an open state. A similar conclusion was also deduced from the differential ligand binding kinetics of rat IFABP and its helix-less variant.[6] On the other hand, the rates for the slow step were nearly independent of ligand concentrations (Figure 2; Supporting Information, Figure S6), implying that this step is a unimolecular reaction. This slow step may correspond to the conformational exchange of the ligand-bound protein from an open state to a closed state. Taken together, the ligand binding can be described by the following three-step model:

$$\mathrm{FABP(closed)} \leftrightarrow \mathrm{FABP(open)}\ \text{(step 1)} \quad (1)$$

$$\mathrm{FABP(open)} + \mathrm{L} \leftrightarrow \mathrm{FABP \cdot L(open)}\ \text{(step 2)} \quad (2)$$

$$\mathrm{FABP \cdot L(open)} \leftrightarrow \mathrm{FABP \cdot L(closed)}\ \text{(step 3)} \quad (3)$$

At 20 °C, the maximum forward rate of step 1 for hIFABP (ca. 1100 s^{-1}) was about four times as large as that of the variant in the presence of the disulfide bond (280 s^{-1}), while the forward rate of step 3 for hIFABP was about three times as large as that of the variant (Supporting Information, Figure S6). The results demonstrate that the disulfide bond significantly slows down the conformational exchange processes of both the ligand-free and ligand-bound proteins. As expected, the binding process was decelerated by decreasing temperature and the kinetic features at different temperatures remained the same (Figure 2; Supporting Information, Figures S4–S6). At 13 °C, the maximum forward rate of step 1 for the variant was 180 s^{-1}, while the forward rate of step 3 was about 5 s^{-1}, and both were smaller than those at 20 °C.

To understand the conformational exchange, we carried out NMR relaxation dispersion experiments[19,20] on the ligand-free mutant with a disulfide bond at 13 °C. In total, 93 and 91 backbone amides displayed obvious ^{1}H and ^{15}N relaxation dispersion (Figure 3; Supporting Information, Figure S7), respectively. The ^{15}N dispersion profile for each available residue could be fitted nicely to a two-state exchange model ($N \overset{k_{ex1}}{\rightleftarrows} I1$). The ^{1}H dispersion profiles for most residues could also be fitted to the same two-state model, but 21 profiles could not be fitted in the same way. Since the residues displayed obvious ^{15}N relaxation dispersion

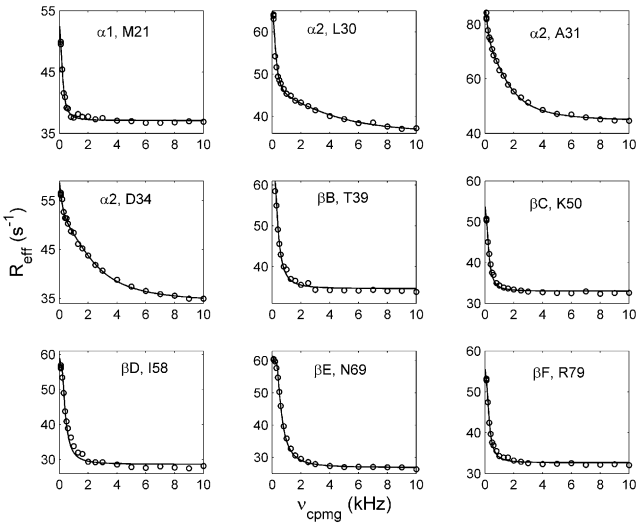

Figure 3. Representative ^{1}H relaxation dispersion profiles of the hIFABP variant with a disulfide bond. The experimental data are indicated by ○, while the solid lines are best fits obtained with a two-state model (M21,T39, K50, I58, N69, and R79) or three-state model (L30, A31, and D34).

are distributed over all the β strands and helices (Figure 1B), a global two-state exchange process should exist. Combining the ^{15}N dispersion data with the ^{1}H dispersion profiles that could be fitted to the two-state model, we determined the exchange rate ($k_{ex1} = 1072 \pm 22\ s^{-1}$), population of the minor state ($P_{I1} = 3.53 \pm 0.02\,\%$), and chemical shift differences of ^{1}H and ^{15}N spins between the major native state N and minor state I_1 ($|\delta_N - \delta_{I1}|$) (Supporting Information, Table S2). The conversion rate from the closed state N to state I_1 was about $38\ s^{-1}$, which is much smaller than the forward rate of step 1 described above (ca. $180\ s^{-1}$). This conformational exchange process is similar to what we observed previously for liver FABP, which has been demonstrated to be irrelevant to the ligand entry process.[16]

The 21 residues that could not be fitted to the two-state model are located in the second helix (C27–A32, D34) and its proximal region (Figure 1B): Y14, M18, and E19 located in α1, L36 and K37 in the loop between α2 and strand B, V23 in the loop between the two helices, S53 and A54 in the turn C-D, L72 and G75–L78 in the turn E-F, and V8 close to L36 and K37. For these residues, the ^{1}H relaxation rates were dependent on CPMG field strength even when the strength was larger than 4000 Hz (Figure 3), indicating the presence of another conformational exchange process which is much faster than about $1000\ s^{-1}$. Thus, a three-state model is assumed for these residues ($I1 \overset{k_{ex1}}{\leftrightarrow} N \overset{k_{ex2}}{\leftrightarrow} I2$). In this model, the slower exchange process is considered the same as the exchange derived from the two-state model. Fitting these ^{1}H dispersion profiles simultaneously, we obtained the exchange rate between the third state (I_2) and the major closed state ($k_{ex2} = 13382 \pm 512\ s^{-1}$), the population of state I_2 ($1.45 \pm 0.06\,\%$), and $|\delta_N - \delta_{I1}|$ and $|\delta_N - \delta_{I2}|$ of ^{1}H spins (Supporting Information, Table S2). According to this result, the transition rate from the closed state to state I_2 is about $195\ s^{-1}$, which is comparable to the forward rate limit of step 1 as determined by the stopped-flow experiments (ca. $180\ s^{-1}$). The excellent correlation indicates that this faster conformational exchange corresponds to the opening process or the rate-limiting step for ligand binding (step 1).

To characterize the structures of minor states I_1 and I_2, their chemical shifts were compared with the native state and the unfolded state at 8 M urea (Supporting Information, Table S2). If a minor state is similar to the native state in structure, the $|\delta_N - \delta_I|$ values of ^{1}H and/or ^{15}N spins should be small. If a minor state is close to the unfolded state, the $|\delta_N - \delta_I|$ values should be similar to the chemical shift differences between the native and the unfolded states ($|\delta_N - \delta_U|$). For most residues in state I_1, the ^{1}H $|\delta_N - \delta_{I1}|$ values were small and were very different from the corresponding values of $|\delta_N - \delta_U|$ (Supporting Information, Table S2), suggesting that state I_1 is a native-like intermediate state. This conclusion is further supported by the observation that the ^{15}N $|\delta_N - \delta_{I1}|$ values for most residues were significantly smaller than the corresponding $|\delta_N - \delta_U|$ values. For most residues in the second helix such as R28, K29, L30, A32, and D34 in state I_2, the ^{1}H $|\delta_N - \delta_{I2}|$ values were large and were also quite close to the corresponding $|\delta_N - \delta_U|$ values (Supporting Information, Table S2), implying that this helix is mainly unfolded in state I_2. On the other hand, most residues in the first helix and nearly all the residues in β-strands did not exhibit the third state I_2. Therefore, state I_2 very likely adopts a locally unfolded conformation, in which only the second helix is largely unfolded. Locally unfolded states were also observed in other proteins.[21] Owing to the unfolding of α2, the residues proximal to this helix can be altered in chemical environments, and thus their chemical shifts in state I_2 are different from those in the native state.

To further examine the structural features of states I_1 and I_2, we conducted hydrogen–deuterium (H-D) exchange experiments. The amides located in α2 and those not involved in hydrogen bonding in the native state were undetectable in the 2D HSQC recorded at pH 7.1 with a total acquisition time of 70 seconds, immediately after putting the sample in the magnet (Supporting Information, Figure S8). For these fast exchange amides, their exchange rates with water (H_2O) were measured using an amide hydrogen exchange technique.[22] Under the EX2 (bimolecular exchange) condition where the local closing rate is much larger than the H-D exchange rate for unprotected amides,[23] the protection factor (P) can be approximated as P_C/P_O, where P_O and P_C are the populations of the open and closed states, respectively. Except for a few amides, the H-D exchange rates measured at pH 7.4 were about 1.5–3 times higher than those at pH 7.1 (Supporting Information, Table S3), demonstrating that the amide hydrogen exchange occurs through an EX2 limit at pH 7.1. If either state I_1 (population of 3.53 %) or state I_2 (population of 1.45 %) was in an entirely unfolded open form, the observed protection factors for all amides would be smaller than 100. However, most amides in α1 and β-strands had protection factors larger than 1000 (Figure 1C), demonstrating that both states I_1 and I_2 are in a mainly folded form, consistent with the relaxation dispersion results. Examining the structure of the cap-closed variant, we found that the amides in V17-M21 (α1) and K29-A32 (α2) form hydrogen bonds and have similar accessibilities to water. If no local unfolding occurs, these amides should have similar H-D exchange rates which are dominated by the accessibility to water and hydrogen bonding of amides. In fact, the protection factors for K29-A32 were smaller than 100, but those for V17-M21 were larger than 10000. The result proves that the second helix experiences local unfolding. For the wild type hIFABP, H-D exchanges for all the amides in helix 2 finished within the dead time by NMR (ca. 180 s), but V17-M21 displayed nearly no peak intensity changes within 1 hour. This result shows that local unfolding of the second helix also occurs for the wild type hIFABP.

In summary, we have demonstrated that the hIFABP variant K27C/D74C exists mainly in a cap-closed conformation through the formation of an intramolecular disulfide bond. This variant still uptakes fatty acids although its cap is closed. Besides the major conformation, K27C/D74C exists in two minor states: one native-like state I_1 and one locally unfolded state I_2 in which the second helix is largely unfolded. The major state is in conformational exchanges with states I_1 and I_2, but only the exchange with the locally unfolded state I_2 is functionally relevant since the transition rate from the closed native state to the locally unfolded state agrees with the maximal ligand association rate. Local unfolding of helix 2

generates an opening to allow ligands such as fatty acids to enter or leave the protein cavity. The locally unfolded state I_2 should also exist in the wild type hIFABP since this protein and its variant behaved similarly in H-D exchange and ligand binding. Because FABPs are highly conserved in 3D structures and ligand binding, all FABPs may use the same local unfolding mechanism for uptaking and releasing ligands.

Acknowledgements

This research was supported by grants from Singapore Ministry of Education (Academic Research Fund Tier 3, MOE2012-T3-1-008; Academic Research Fund Tier 2, MOE2012-T2-2-138). The authors thank Dr. Martin Scanlon for providing the wild-type hIFABP construct.

Keywords: conformational exchange · fatty acid binding proteins · local unfolding · protein dynamics · protein structure

How to cite: *Angew. Chem. Int. Ed.* **2016**, *55*, 6869–6872
Angew. Chem. **2016**, *128*, 6983–6986

[1] L. Ragona, K. Pagano, S. Tomaselli, F. Favretto, A. Ceccon, S. Zanzoni, M. D'Onofrio, M. Assfalg, H. Molinari, *Biochim. Biophys. Acta Proteins Proteomics* **2014**, *1844*, 1268–1278.
[2] M. Furuhashi, G. S. Hotamisligil, *Nat. Rev. Drug Discovery* **2008**, *7*, 489–503.
[3] J. C. Sacchettini, J. I. Gordonl, L. J. Banaszak, *J. Mol. Biol.* **1989**, *208*, 327–339.
[4] M. E. Hodsdon, D. P. Cistola, *Biochemistry* **1997**, *36*, 1450–1460.
[5] D. Long, Y. Mu, D. Yang, *Plos One* **2009**, *4*, e6081.
[6] D. P. Cistola, K. Kim, H. Hans Rogl, C. Frieden, *Biochemistry* **1996**, *35*, 7559–7565.
[7] J. C. Sacchettini, J. I. Gordon, L. J. Banaszak, *Proc. Natl. Acad. Sci. USA* **1989**, *86*, 7736–7740.
[8] J. Cai, C. Lücke, Z. Chen, Y. Qiao, E. Klimtchuk, J. A. Hamilton, *Biophys. J.* **2012**, *102*, 2585–2594.
[9] J. Thompson, N. Winter, D. Terwey, J. Bratt, L. Banaszak, *J. Biol. Chem.* **1997**, *272*, 7140–7150.
[10] C. Luecke, M. Rademacher, A. Zimmerman, H. T. B. van Moerkerk, J. H. Veerkamp, H. Rueterjans, *Biochem. J.* **2001**, *354*, 259–266.
[11] Y. Xu, D. Long, D. Yang, *J. Am. Chem. Soc.* **2007**, *129*, 7722–7723.
[12] Y. He, X. Yang, H. Wang, R. Estephan, F. Francis, S. Kodukula, J. Storch, R. E. Stark, *Biochemistry* **2007**, *46*, 12543–12556.
[13] M. E. Hodsdon, D. P. Cistola, *Biochemistry* **1997**, *36*, 2278–2290.
[14] L. H. Gutiérrez-González, C. Ludwig, C. Hohoff, M. Rademacher, T. Hanhoff, H. Rüterjans, F. Spener, C. Lücke, *Biochem. J.* **2002**, *364*, 725–737.
[15] C. Lücke, D. Fushman, C. Ludwig, J. A. Hamilton, J. C. Sacchettini, H. Rüterjans, *Mol. Cell. Biochem.* **1999**, *192*, 109–121.
[16] D. Long, D. Yang, *Biophys. J.* **2010**, *98*, 3054–3061.
[17] Y. Xu, Y. Zheng, J. Fan, D. Yang, *Nat. Methods* **2006**, *3*, 931–937.
[18] D. Yang, Y. Zheng, D. J. Liu, D. F. Wyss, *J. Am. Chem. Soc.* **2004**, *126*, 3710–3711.
[19] R. Ishima, P. T. Wingfield, S. J. Stahl, J. D. Kaufman, D. A. Torchia, *J. Am. Chem. Soc.* **1998**, *120*, 10534–10542.
[20] B. Jiang, B. Yu, X. Zhang, M. Liu, D. Yang, *J. Magn. Reson.* **2014**, *257*, 1–7.
[21] J. Lim, T. Xiao, J. Fan, D. Yang, *Angew. Chem. Int. Ed.* **2014**, *53*, 2358–2361; *Angew. Chem.* **2014**, *126*, 2390–2393.
[22] J. Fan, J. Lim, B. Yu, D. Yang, *J. Biomol. NMR* **2011**, *51*, 151–162.
[23] M. M. Krishna, L. Hoang, Y. Lin, S. W. Englander, *Methods* **2004**, *34*, 51–64.

Received: February 5, 2016
Revised: March 18, 2016
Published online: April 23, 2016

